

DEUTSCHES ELEKTRONEN-SYNCHROTRON **DESY**

DESY 82-083
December 1982



TWO-PHOTON INTERACTIONS

by

Dieter Cords

ISSN 0418-9833

NOTKESTRASSE 85 · 2 HAMBURG 52

DESY behält sich alle Rechte für den Fall der Schutzrechtserteilung und für die wirtschaftliche Verwertung der in diesem Bericht enthaltenen Informationen vor.

DESY reserves all rights for commercial use of information included in this report, especially in case of filing application for or grant of patents.

To be sure that your preprints are promptly included in the
HIGH ENERGY PHYSICS INDEX ,
send them to the following address (if possible by air mail) :

DESY
Bibliothek
Notkestrasse 85
2 Hamburg 52
Germany

TWO-PHOTON INTERACTIONS*

Dieter Cords
DESY, Hamburg

Two-photon interactions are obtained at high energy electron positron storage rings. The cross section for the process, illustrated by diagram 1, can be factorized in the equivalent photon approximation^{1,2)} into a flux factor and into the actual two-photon cross section:

$$\begin{aligned} d\sigma(e^+e^- \rightarrow e^+e^- \gamma_1 \gamma_2 \rightarrow e^+e^- X) \\ \approx dN_{\gamma_1} dN_{\gamma_2} \sigma(\gamma_1 \gamma_2 \rightarrow X) \end{aligned}$$

Abstract

Recent spectroscopic results on f , A_2 , and f' are reviewed and the suppression of the glueball candidate state ϕ in the two-photon channel is discussed. A newly observed signal in the $\pi^+ \pi^+ \pi^- \pi^-$ invariant mass spectrum at 2.1 GeV is reported. Measurements on deep inelastic $e\gamma$ scattering show the expected pointlike photon structure and allow to test the photon structure function F_2 for parton and QCD models. The observation of high P_T jets from hard scattering processes is presented.

* Talk presented at the 1982 SLAC Summer Institute on Particle Physics.

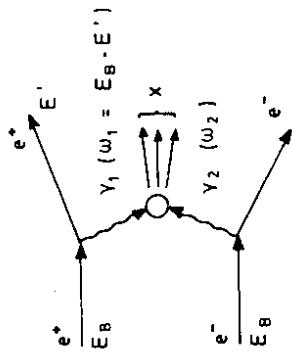


Diagram 1

where dN_{γ} gives the number of photons in the energy interval between ω and $\omega+d\omega$. The flux factor can be used to relate the e^+e^- annihilation luminosity to the two-photon luminosity³⁾:

$$\begin{aligned} dL_{\gamma\gamma} &= dN_{\gamma_1} dN_{\gamma_2} L_{e^+e^-} \\ &\approx \left(\frac{2\alpha}{\pi}\right)^2 \ln \frac{E_B}{m_e} \frac{d\omega_1}{\omega_1} \frac{d\omega_2}{\omega_2} L_{e^+e^-} \\ &\sim \frac{1}{400} \frac{d\omega_1}{\omega_1} \frac{d\omega_2}{\omega_2} L_{e^+e^-} \quad \text{for } E_B = 15 \text{ GeV}. \end{aligned}$$

The suppression of the two-photon luminosity by a factor of about 400 at present beam energies is compensated by the fact that the approximate⁴⁾ two-photon cross section $\sigma(\gamma\gamma \rightarrow \text{hadrons}) \approx 300 + \frac{600}{W(\text{GeV})} \text{nb}$

is much larger than the annihilation cross section $\sigma(e^+e^- \rightarrow \text{hadrons}) \approx 0.5 \text{ nb}$. Therefore, the event rate for two-photon interactions is expected to be larger than the rate for e^+e^- annihilation processes at PEP and PETRA energies. However, since most of the two-photon events are produced at low invariant masses, they may not produce sufficient transverse energy to trigger the detector and therefore suffer from acceptance problems. If in addition the electron or positron is required to be tagged⁵⁾ in a typical angular range from 25 to 70 mrad with respect to the beam line, the event rate decreases further by about a factor of 10.

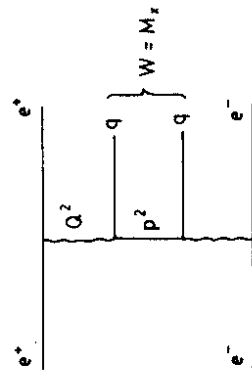


Diagram 2

If - in analogy to e^+e^- annihilation - the hadron production is represented by quark lines, one can use the four-momentum transfers Q^2 and P^2 , indicated in diagram 2, to classify the various possible processes according to different kinematic regions.

kinematic region	physics of interest	experimental method
Q^2 and P^2 soft (~ 0 and $\sim 1 \text{ GeV}^2$)	SPECTROSCOPY & 2-BODY PRODUCTION	exclusive final states with transverse momentum balance $\Sigma p_T^i \neq 0$
Q^2 hard ($\geq 10 \text{ GeV}^2$)	DEEP INELASTIC eY SCATTERING	tagged electrons with $Q^2 = 4E_B E' \sin^2 \theta$ & W measurement
P^2 hard ($\geq 10 \text{ GeV}^2$)	HARD SCATTERING PHENOMENA	Jet analysis for the hadronic system $P^2 \sim P_{q,T}^2 + (\frac{W}{2} - P_{q,L})^2 \leq \frac{W^2}{2}$

For the last process a minimum invariant mass W of about 5 GeV is required. The higher the W values for the selected events, the more likely it is to obtain background events from e^+e^- annihilation where one or both of the electrons radiated off a real photon in the initial state. The decreasing two-photon event rate and the increasing annihilation background reach about the same order of magnitude at a W of approximately half the total available energy.

The processes outlined above will be discussed in the following chapters.

Spectroscopy

The prime objective for analysing resonances in two-photon interactions is to obtain the radiative width $\Gamma_{R\gamma\gamma}$ via the production cross sections:

$$\frac{d\sigma(e^+e^- \rightarrow e^+e^-R)}{dM} = L_{\gamma\gamma} \left(\frac{M}{2E_B}\right) \sigma_{\gamma\gamma \rightarrow R}(M) \frac{1}{2E_B}$$

$$\text{with } \sigma_{R \rightarrow \gamma\gamma} = 8\pi(2J+1) \frac{\Gamma_{R\gamma\gamma} \Gamma}{(M^2 - M_R^2)^2 + M_R^2 \Gamma^2}$$

where M is the invariant mass of the two-photon system, J the spin, and $L_{\gamma\gamma}$ the luminosity function⁶⁾. The well defined initial state restricts the resonance quantum numbers to:

$$I_3 = 0, J^{PC} = 0^{-+}, 0^{++}, 2^{-+}, 2^{++}, \dots$$

where spin 1 states are excluded for nearly real photons. In this way one can investigate the isoscalar components of scalar and tensor meson nonets. The questions of interest are whether these resonances are pure quark bound states or have some gluonium admixture, and at what level do we expect glueball states to be produced if these states exist at all. It would also be interesting to look for even C-parity charmonium states, e.g. η_c, χ_0, χ_2 , but there are no measurements yet.

In recent years many nice results on two-photon resonances have been obtained and surveys were presented at various conferences^{7,8)}.

In this report I shall discuss the neutral members f, A_2^0 , and f' of the 2^{++} meson nonet. The measured radiative widths for various decay modes are summarized in Fig. 1. As shown by the squares linked by dashed lines, $SU(3)$ for ideal mixing and without phase space corrections predicts ratios (not absolute values) of radiative widths which are in fair agreement with the averaged measurements.

An example for the f decay into two charged pions⁹⁾ is given in Fig. 2a showing the TASSO invariant mass spectrum for two charged tracks. Since electrons, muons, and pions cannot be separated at low momenta, the QED contribution (dotted line) has to be subtracted. The QED subtracted invariant mass distribution in Fig. 2b shows in addition to the f signal at 1.27 GeV a strong enhancement near threshold. This can be contrasted with the $\pi^0\pi^0$ spectrum¹⁰⁾ in Fig. 3 obtained by the JADE collaboration which shows an f signal over a very small background. An example for a final state with charged and neutral particles is the A_2^0 decay¹¹⁾ which is illustrated in Fig. 4. The hatched area indicates the dominant decay mode into $\rho^+\pi^-$. The f' signal¹²⁾ has been seen by the TASSO collaboration at 1.52 GeV in the K^+K^- and $K_S^0K_S^0$ final states (Fig. 5). Whereas one observes the expected constructive interference of the f' with f and A_2 as a strong enhancement below the f' mass for charged kaons, this is neither expected nor seen for neutral kaons.

It is well known that the radiative decays of the J/ψ resonance allow the formation of two-gluon states¹³⁾ of even C-parity and

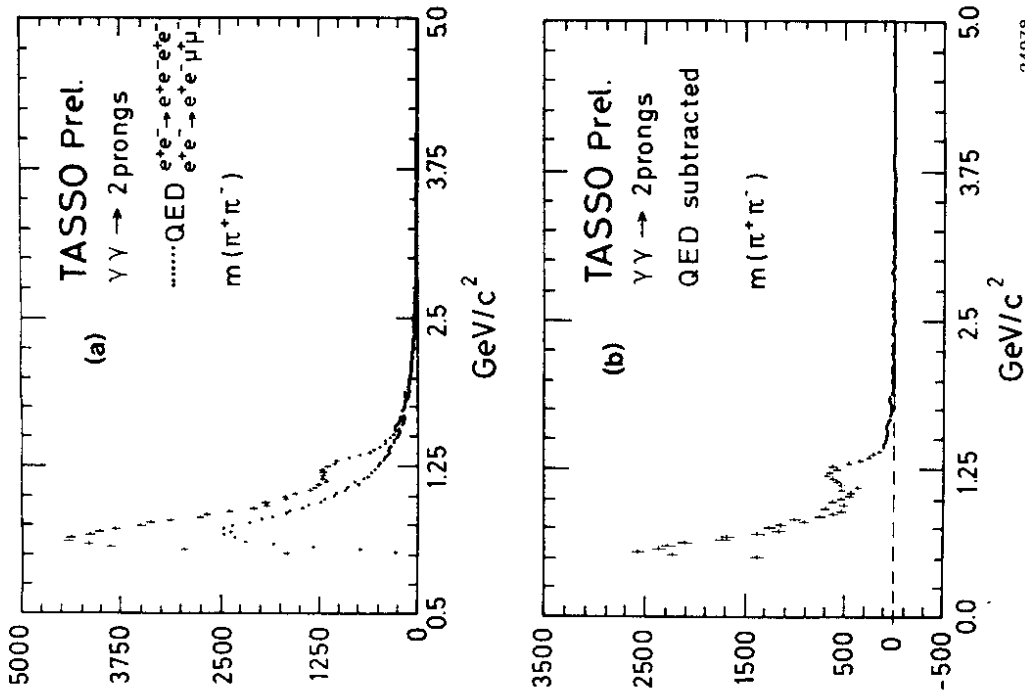


Fig. 2 : Invariant $\pi^+\pi^-$ mass from TASSO (a) for all events with 2 charged tracks and (b) after QED - i.e. $\mu^+\mu^-$ and e^+e^- subtraction.

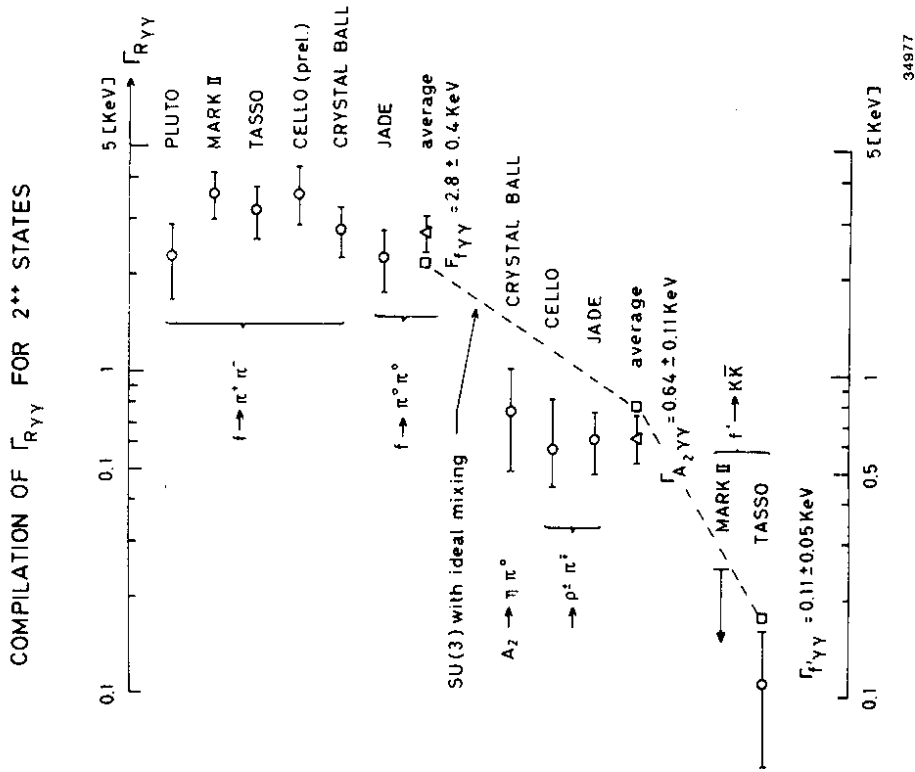


Fig. 1 : Compilation of radiative widths for the f , A_2 , and f' resonances. For references see J. Olsson⁸⁾ and ref. 12. The average values are given numerically. $SU(3)$ for ideal mixing - fixing the ratios but not the absolute values - is indicated by the dashed lines.

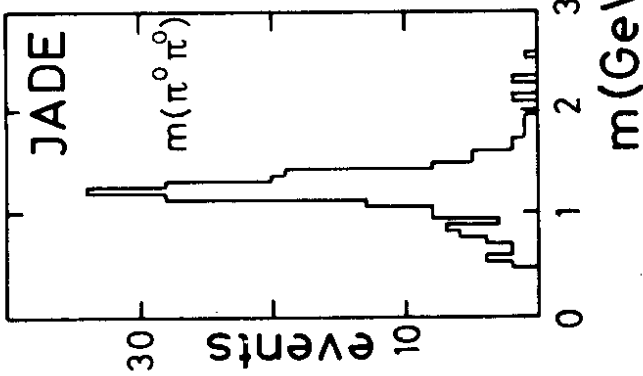
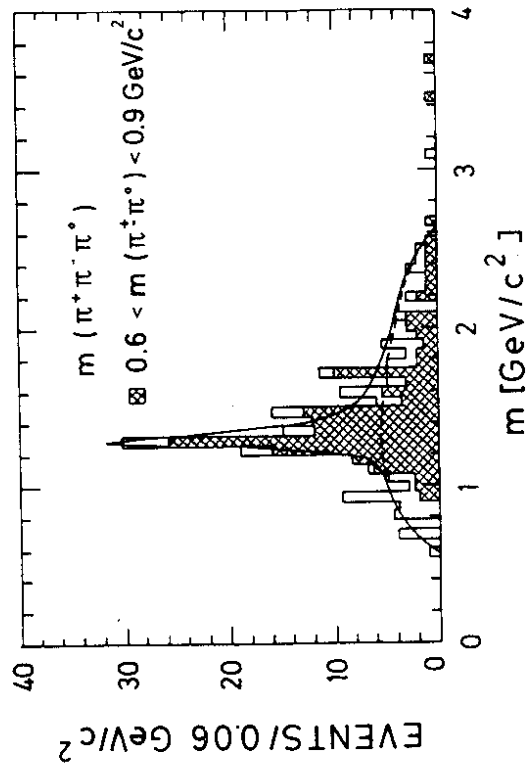


Fig. 3 : Invariant $\pi^+\pi^-\pi^0$ mass from JADE.

Fig. 4 : Invariant $\pi^+\pi^-\pi^0$ mass from JADE. The cross-hatched histogram presents the dominant $\rho^+\pi^+$ decay mode of the A_2 .



33929

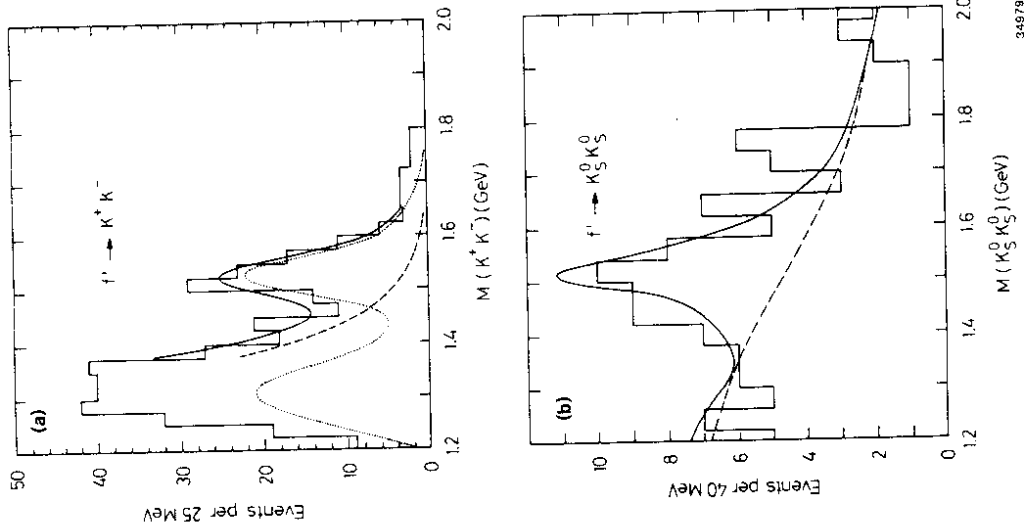


Fig. 5 : Invariant $K\bar{K}$ mass from TASSO:
 (a) $M(K^+K^-)$ distribution. The dotted curve is the contribution from the interfering f_2 , A_2 , and f' resonances. The background is given by the dashed line. The full curve is the sum of both contributions.
 (b) $M(K_S^0 K_S^0)$ distribution. The full curve is the result of a fit to a background (dashed line) plus a Breit-Wigner shaped :

therefore are called "glueball-favoured". On the other hand the production of even C-parity states via two photons is called "glueball-disfavoured" because one has to insert an extra quark loop as shown

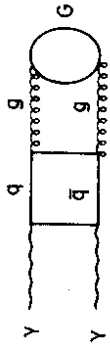


Diagram 3

by diagram 3. One may guess

that the suppression factor

in the two-photon case is the

square root of the Okubo-

Zweig-Iisuka-factor¹⁴ which involves two quark loops and is about

1/100. Applying this to the glueball candidate state θ , observed¹⁵

at 1.64 GeV in various decay channels, one can obtain its two-photon width from the corresponding value for the f' :

$$\frac{\Gamma(\theta \rightarrow \gamma\gamma)}{\Gamma(f' \rightarrow \gamma\gamma)} \approx \left[\frac{M_\theta}{M_{f'}} \right]^3 \cdot \sqrt{ZI} = 0.2$$

Using the radiative f width of Fig. 1, this results in $\Gamma(\theta \rightarrow \gamma\gamma) \sim$

600 eV. Mark II¹⁶ has recently measured the branching fraction

$BR(J/\psi \rightarrow \gamma\theta) \cdot BR(\theta \rightarrow K^+K^-) = (6.2 \pm 2.7) \cdot 10^{-4}$. According to gluo-

nic duality arguments Koller and Walsh¹⁷ estimated the branching

ratio $BR(J/\psi \rightarrow \gamma\theta) \approx 2\%$, and therefore one expects $BR(\theta \rightarrow K^+K^-) \approx 3\%$.

Using the last value together with the estimated radiative θ width one expects the following signal in the two-photon case:

$$\Gamma(\theta \rightarrow \gamma\gamma) \cdot BR(\theta \rightarrow K^+K^-) \sim 20 \text{ eV}$$

Since θ is three times as wide as the f' , one is looking for an enhancement in the K^+K^- invariant mass spectrum (Fig. 5) which is less than 1/10 of the f' peak. In fact the TASSO upper limit¹² is 0.5 KeV (95% c.l.). Similar results apply to the $\rho\rho$ decay of the θ . Therefore,

in addition to not being firmly established as glueball states, the θ as well as the i are below the level of detection for present two-photon experiments.

An interesting conjecture of Schnitzer¹⁸ and Rosner¹⁹ implies that glueballs are not pure gluonium but contain some admixture of quarkonium states. This means that glueballs might mix with the isoscalar nonet members and as a consequence their coupling to the two-photon channel might be quite different from the estimate given above. However, at this preliminary stage I shall not pursue the question further.

A new enhancement²⁰ has been observed by the TASSO collaboration in the final state of 4 charged pions. Fig. 6 shows the invariant mass spectrum of the reaction $\gamma\gamma \rightarrow \pi^+ \pi^+ \pi^- \pi^-$ for an accumulated luminosity of 70 pb^{-1} . A signal of about 5 standard deviations can be seen at 2.1 GeV. A fit of a Gaussian distribution over a smooth background is shown in the lower histogram and results in a mass of $2.10 \pm 0.01 \text{ GeV}$ and a full width at half maximum of $94 \pm 21 \text{ MeV}$. The mass resolution is estimated to be 60 MeV, and therefore the actual width is much less than measured. The two-photon coupling times the branching ratio of this state X of unknown spin J is given as:

$$\Gamma(X \rightarrow \gamma\gamma) \cdot BR(X \rightarrow \pi^+ \pi^+ \pi^- \pi^-) \cdot (2J + 1) = 1.6 \pm 0.4 \text{ KeV}$$

Since the spin and parity of this object are not determined, one cannot discuss any multiplet assignment. However, one may speculate whether this enhancement is related to a strong signal near the

threshold of the $\phi\phi$ invariant mass spectrum²¹⁾ shown in Fig. 7 for the reaction $\pi^-\text{Be} \rightarrow \phi\phi + \dots$ at 175 and 100 GeV/c. Recently the observation of two $\phi\phi$ resonances²²⁾ in the reaction $\pi^-\text{p} \rightarrow \phi\phi\text{n}$ was reported at the Paris conference. The quantum numbers are quoted as $J^G = 0^+$ and $J^{PC} = 2^{++}$ for both states and the lower mass state has $M = 2.16 \pm 0.04$ GeV and $\Gamma = 315 \pm 62$ MeV. Compared to the enhancement in the two-photon case it is very wide. The special interest in $\phi\phi$ states arises from the idea that the production of these strange quark states is mediated by two gluons and can be enhanced only if the gluons form a resonance or glueball. For further details the reader is referred to Sharre's report on glueballs²³⁾.

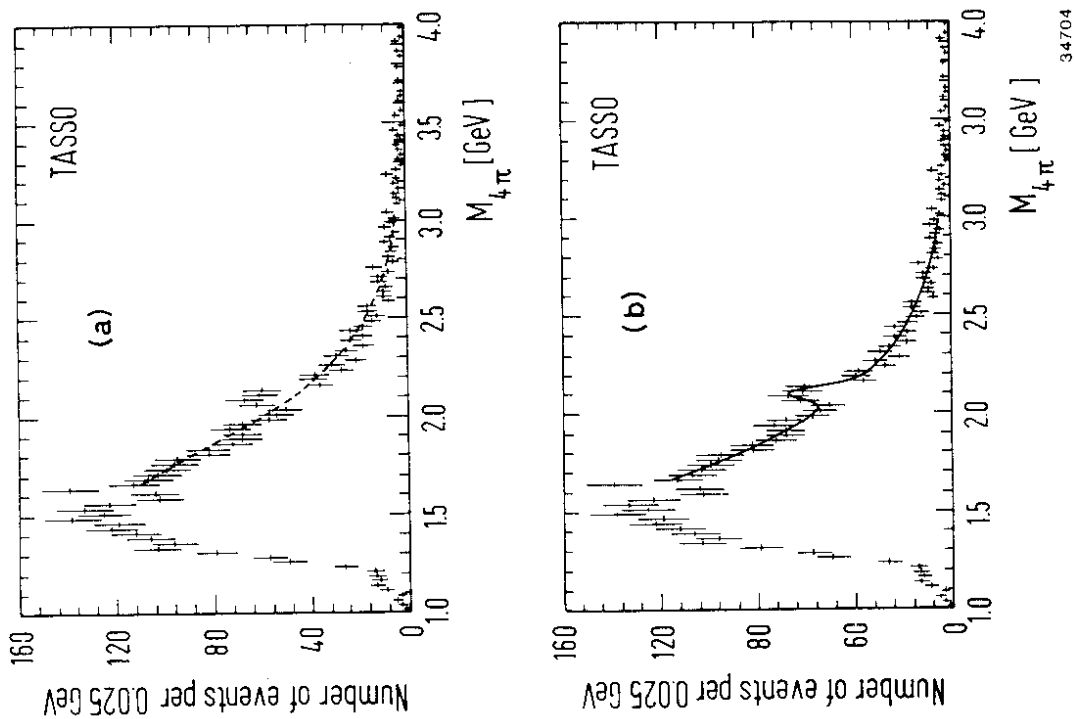


Fig. 6 : Invariant $\pi^+\pi^-\pi^+\pi^-$ mass from TASSO. The curve in (b) represents the fit of a Gaussian superimposed on a smooth background.

Two-Body Final States

Results on two-body final states have been reported before^{7,8)} and therefore I shall be very brief. It is well known that the four charged pion final state up to an invariant mass of 2 GeV is dominated by $\rho^0\rho^0$ production. Recently TASSO²⁴⁾ has performed an angular correlation analysis for the $\rho^0\rho^0$ channel and found that $J^P = 0^-$ and 2^- states can be excluded within experimental accuracy. The contributions mainly come from $J^P = 0^+$ below an invariant mass of 1.7 GeV and from $J^P = 2^+$ above. The cross section somewhat depends on the assumptions put into the fitting procedure. As shown in Fig.8, it is substantially higher if the ρ 's are assumed to be produced and to decay isotropically.

The production of proton antiproton pairs^{8,25)} has been observed by JADE and TASSO, and the cross section near the threshold is found to be smaller than the Born term expectation and larger than the vector dominance model contributions. Recent QCD calculations²⁶⁾ roughly agree with the data although they come out slightly too small very close to threshold.

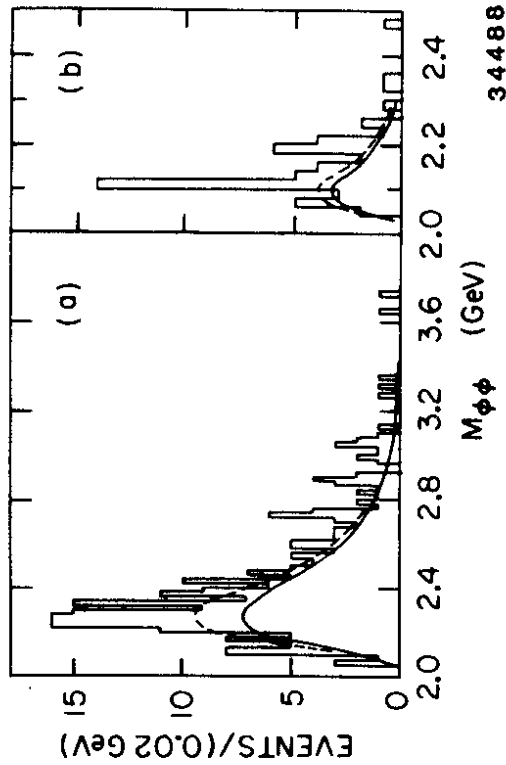


Fig. 7 : Invariant $\phi\phi$ mass from ACCMOR for $\pi^-Be \rightarrow \phi\phi + X$ at (a) 175 GeV and (b) 100 GeV/c. The solid curves show the expected backgrounds from $\phi K^+ K^-$ and $K^+ K^- K^+ K^-$ events. The dashed curves represent the total backgrounds including the estimated contributions from uncorrelated $\phi\phi$ production.

Deep Inelastic e γ Scattering

If one of the photons in diagram 4 is highly virtual and the other is close to mass shell, the process can be seen as deep inelastic electron scattering off a real photon²⁷⁾.

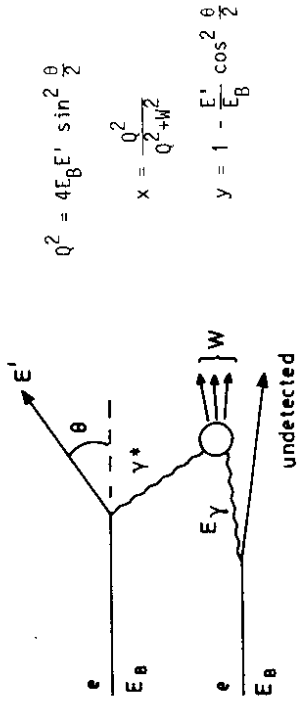


Diagram 4

The two-photon centre-of-mass energy W is measured via the final state products. Q^2 being the spacelike four-momentum-squared of the virtual photon and x, y the standard scaling variables, the differential cross section can be expressed in terms of structure functions^{1,28)}:

$$\frac{d^2\sigma}{dx dy} = \frac{16\pi\alpha^2}{Q^4} E_B E_Y \{ (1-y)F_2(x, Q^2) + xy^2 F_1(x, Q^2) \}$$

In general the cross section depends on three structure functions. However, F_3 drops out if the azimuthal dependence is integrated over (the second electron is not detected). For tagging angles of present experiments, y^2 is a small number - in the range of 0.01 to 0.1 - and as a result the F_1 term can be neglected as well. Therefore,

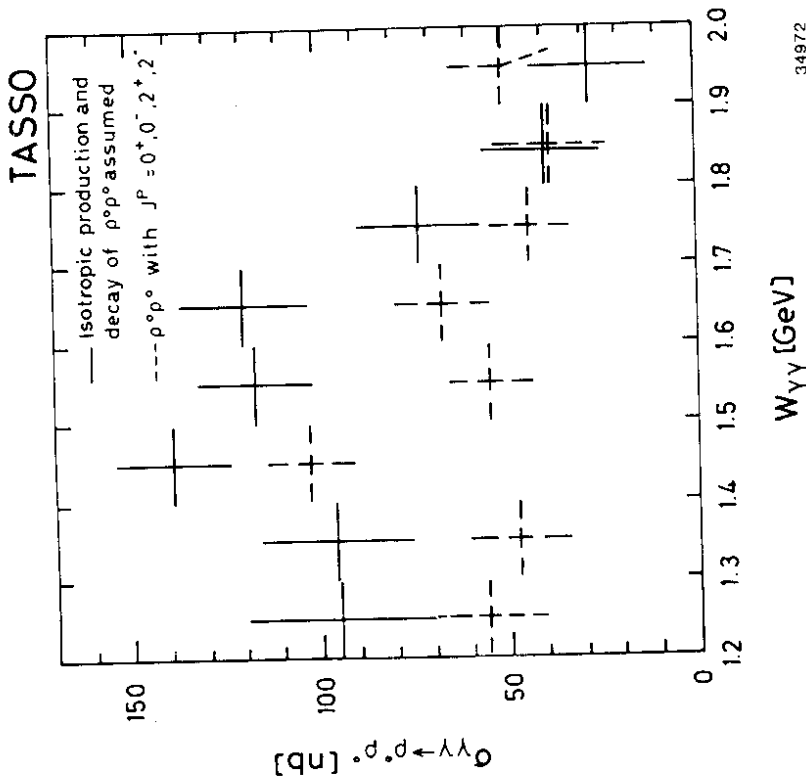


Fig. 8 : Cross section for $\gamma\gamma \rightarrow \rho^0 \rho^0$ from TASSO. For the full crosses the efficiency is calculated assuming isotropic $\rho^0 \rho^0$ production and decay. The dashed crosses represent the sum of different contributions from a spin parity analysis.

the present objective for studying deep inelastic $e\nu$ scattering is to test model predictions by means of the structure function F_2 .

The simplest model for F_2 is the Born term model^[28,29] which applies for lepton pair production and is illustrated by the dash-dotted curve in diagram 5. The characteristic pointlike behaviour in this case is manifested by the large values of F_2^{BORN} for large x .

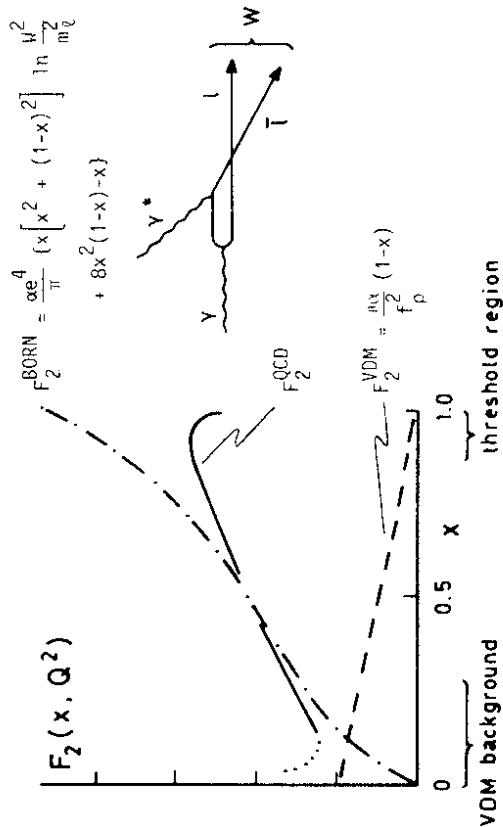


Diagram 5

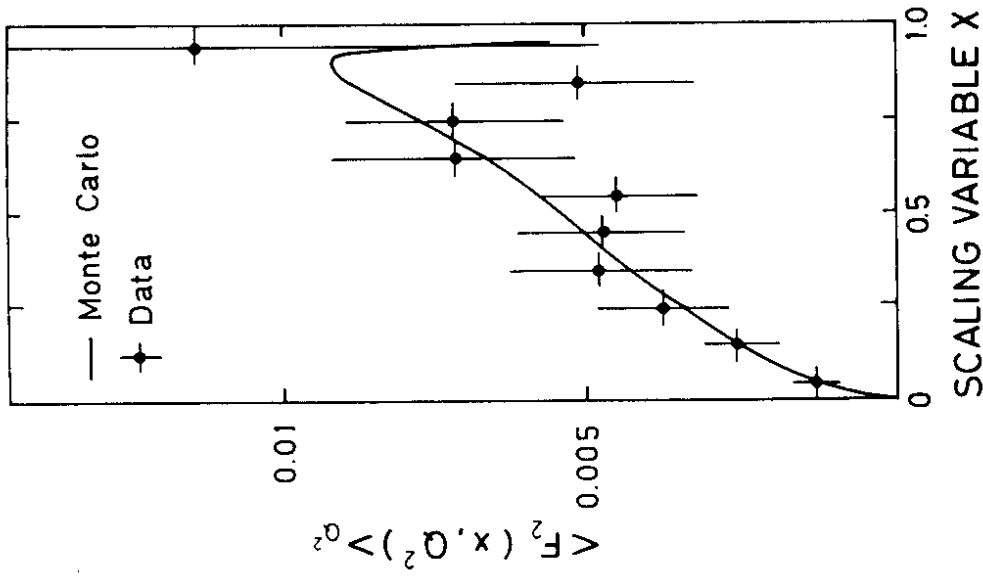
On the other hand, as shown by the dashed line for hadron production in the concept of the vector dominance model^[28], F_2^{VDM} drops off steadily to zero. The question of interest is: Do the hadron production data display a pointlike behaviour in addition to the vector dominance contribution? If that is so, the quark-parton model may be applied. The structure function in the quark-parton model is

obtained from the above Born term by replacing e^4 by the sum of the quark charges to the fourth power and m_l by the quark mass. Therefore, the expected F_2 is very similar in shape to the dash dotted curve. In fact, the theory to be tested is QCD, in which case the structure function is written as:

$$F_2^Y(x, Q^2) = F_2^{\text{QCD}} = \frac{3\alpha_s e_l^4}{\pi} f^{\text{QCD}}(x) \ln \frac{Q^2}{\Lambda^2} + \text{higher order corrections}$$

where e_l are the quark charges, f^{QCD} resembles the x dependence^[30] of the Born term, and the scale parameter Λ replaces the quark mass. A typical QCD behaviour is shown by the solid curve in diagram 5. It has to be pointed out that the higher order QCD corrections^[31,32] show the largest variations in the small x and large x regions. As indicated in diagram 5, the small x region is also the region where the VDM contribution is largest. At large x one enters a threshold region of small W values. Therefore, QCD is best tested in the x range from 0.3 to 0.9. The salient feature of QCD is that it retains the pointlike behaviour of the quark-parton model, i.e. $F_2^Y(x, Q^2) \rightarrow \text{const.}$ as $x \rightarrow 1$ at fixed Q^2 . On the contrary, the proton structure function tends to zero in this case^[33]: $F_2^p(x, Q^2) \sim (1-x)^n \rightarrow 0$.

The Born approximation can be tested for two-photon production of μ -pairs, and a comparison done in Fig. 9 by the CELLO collaboration^[34] shows excellent agreement with the data. The structure function for hadron production has first been obtained by PLUTO^[35] as shown in Fig. 10 for an integrated luminosity of 2500 nb^{-1} . The leading order



34973

Fig. 9 : Comparison of F_2^{BORN} for $e\gamma \rightarrow e\mu^+\mu^-$ with CELLO data (absolute normalization). The F_2 values have been averaged over the Q^2 distribution of the CELLO tagging acceptance.

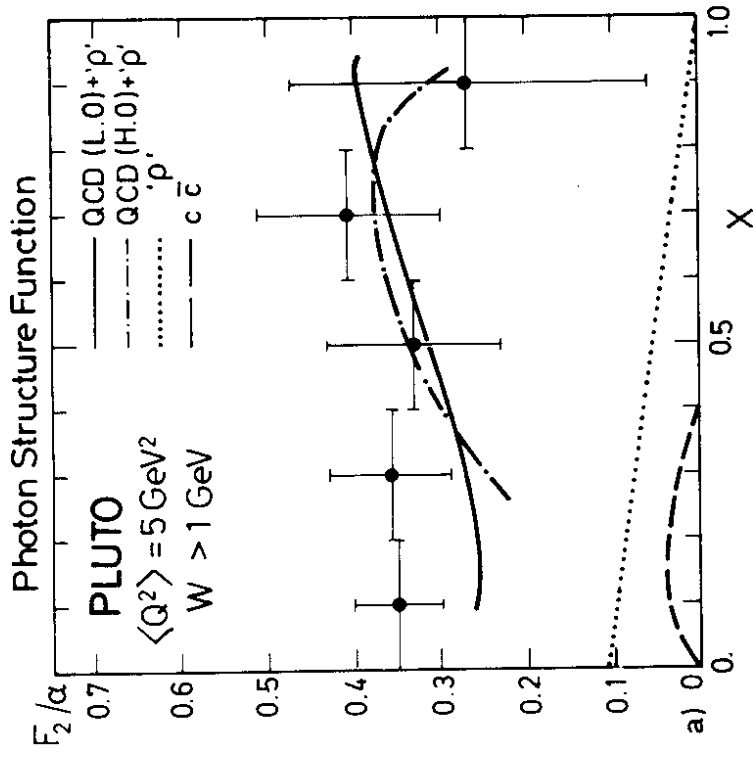
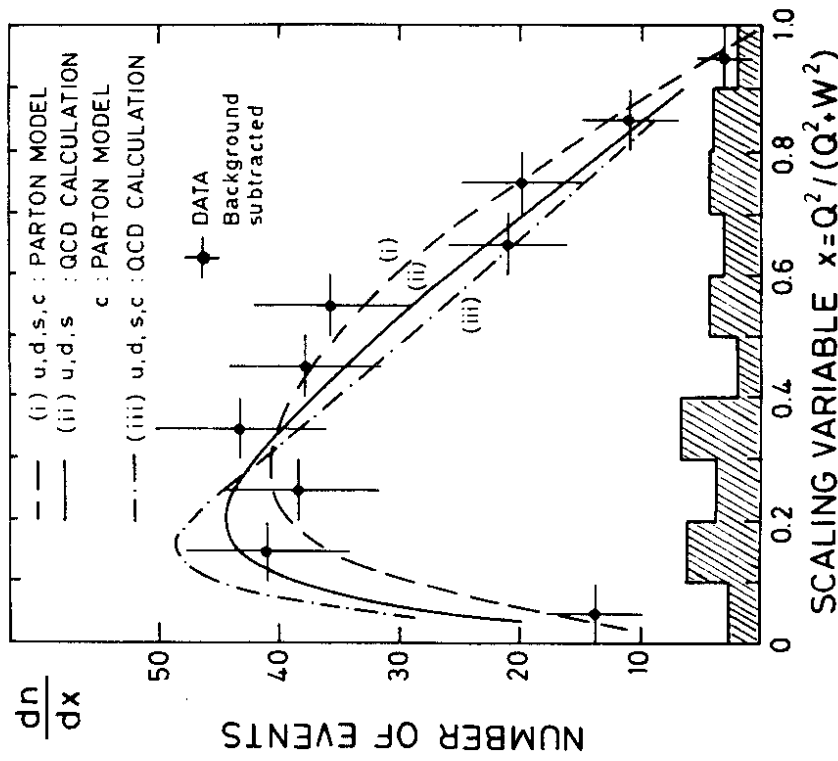


Fig. 10: Photon structure function $F_2(x)/\alpha$ from PLUTO. The various curves correspond to F_2^{QCD} with $\Lambda = 0.2 \text{ GeV}$, F_2^{YDM} for ρ' , and F_2^{BORN} for $c\bar{c}$ with $M_c = 1.5 \text{ GeV}$.

and higher order QCD calculations both agree well with the data and the charm contribution is shown to be small. The data points in Fig. 10 are model dependent because the true x is obtained from the experimentally visible x and this already implies a knowledge of the contributing processes. The average Q^2 in the case of PLUTO is rather low. It mainly depends on the angular range used for tagging one of the electrons and is shown for the three relevant experiments in the following table:

Experiment	Angular range (m rad)	Q^2 range (GeV ²)	$\langle Q^2 \rangle$ (GeV ²)
PLUTO	Large Angle Tagger 100 - 250	1 - 15	5
CELLO	Endcap Liquid Argon 140 - 400	2 - 30	9
JADE	Endcap Lead Glass 265 - 428	10 - 52	23

Unfolding the visible x to obtain the true x - for a direct comparison of the data with the functional dependence of F_2 - already implies a knowledge of F_2 . In order to avoid a simultaneous parameter dependence of the data points and of the models, the data for CELLO and JADE are plotted as a function of the visible x . As a result, the curves for the various models do not exhibit the original x dependence but are folded with the detector acceptance. Fig. 11 shows a comparison of the parton model and two versions of QCD calculations with the CELLO data³⁴⁾ for an integrated luminosity of 11.2 pb^{-1} . Charm quark contributions are included, since



34974

Fig. 11: Visible x distribution from CELLO. The data are compared to three different Monte-Carlo simulations for F_2 . The shaded area shows the background which has been subtracted from the data.

the invariant mass values W extend well above charm threshold. The curves in Fig. 11 are not very different in shape, and at the present level of experimental accuracy it is impossible to distinguish between the parton model and QCD calculations on the basis of the contour of the x distribution. Both models describe the data rather well.

How about the normalization of the structure functions? Considering only the leading order or logarithmic term of F_2^{QCD} above, the normalization depends on the number of quarks included in the charge factor and on the scale parameter Λ . Varying these parameters, a comparison has been done in Fig. 12 to the JADE data³⁶⁾ for an integrated luminosity of 20.2 pb^{-1} . If the u, d, s , and c quarks are included in the leading order QCD term, the full curve in Fig. 12 shows that the scale parameter has to be adjusted to 0.3 GeV to fit the data. This situation roughly corresponds to the parton model with an assumed quark mass of 300 MeV in which case not only the shape but also the normalization seems reasonable. Omission of the charm quark from the leading order QCD term has to be compensated by larger values of $\ln \frac{Q^2}{\Lambda^2}$. As shown by the dashed curve, Λ has to drop in this case to 0.07 GeV . A proper comparison with QCD calculations has to include the charm quark because of the high W values involved and it also has to take higher order QCD corrections into account. In fact, the dotted curve in Fig. 12 includes the next to leading order QCD term³²⁾ in the \overline{MS} scheme³⁷⁾. By varying the scale parameter in the x range above 0.4 , where the VDM contribution is smallest, one obtains for the JADE data³⁶⁾ a best fit of

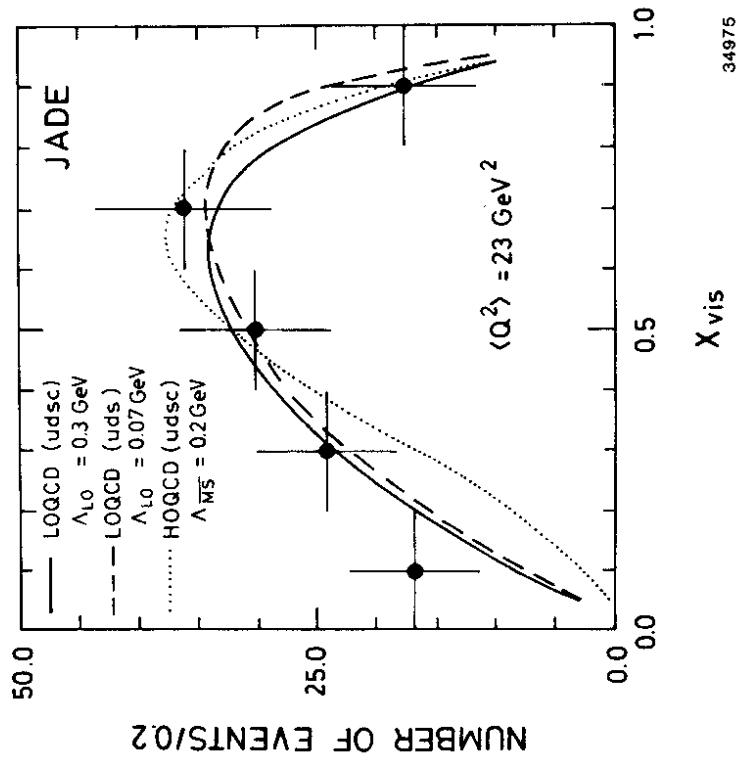


Fig. 12: Visible x distribution from JADE. The curves represent various QCD predictions (see text).

$$\Lambda_{\overline{MS}} = 0.22^{+0.10}_{-0.07} \text{ GeV.}$$

The Q^2 dependence of the structure function is very smooth and given in leading order by $\ln \frac{Q^2}{\Lambda^2}$. In order not to introduce any artificial Q^2 dependence due to detector acceptance, a comparison with the data has to be restricted to that x range where $\langle Q^2 \rangle$ is constant. In Fig. 13 the expected agreement can be observed for PLUTO data³⁵⁾ ($0.2 < x_{vis} < 0.8$) up to Q^2 values of 15 GeV^2 and for JADE data³⁶⁾ ($0.3 < x_{vis}$) up to Q^2 values of 45 GeV^2 .

Since structure functions are an important issue of two-photon physics, let me repeat the relevant points:

- The test of QCD is connected to the dominance of the pointlike term.
- The determination of the QCD scale parameter is done via the normalization of F_2^Y , but one can adjust the average quark mass such that also the parton model fits the data.
- An experimental problem consists in unfolding the visible W or visible x , because this implies a knowledge of the contributing processes and therefore is model dependent.
- There are several problems³⁸⁾ connected to the QCD calculations: The effect of quark masses - in particular for the c quark - has not yet been taken into account. It is an open question, how fast - if at all - the perturbative series of higher order corrections does converge. In this context it is not clear, whether the argument of the logarithm is just Q^2 or whether it contains some additional x dependence.

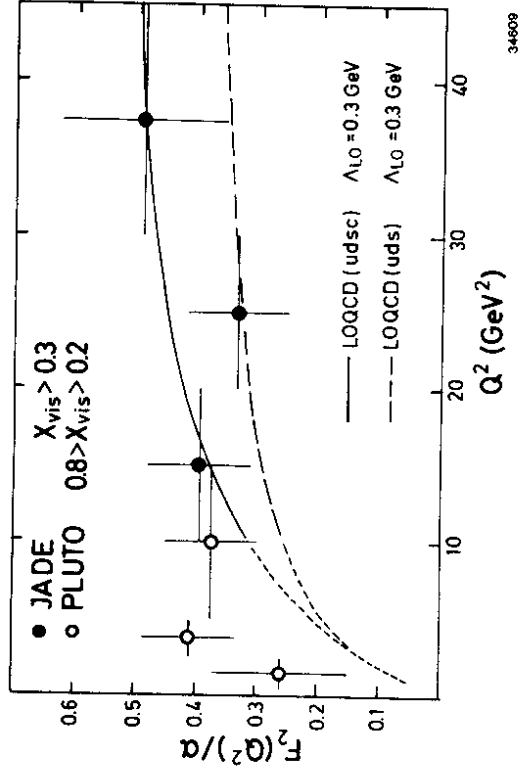


Fig. 13: Photon structure function $F_2(Q^2)/\alpha$ averaged over $x_{vis} > 0.3$ for JADE and over $0.2 < x_{vis} < 0.8$ for PLUTO.

Hard Scattering Phenomena

Hard scattering processes³⁹⁾ are characterized by the fact that a number of particles are produced at high transverse momenta with respect to the line of collision of the initial photons. One can think of several competing processes, like two or more jet events, higher twist terms, and vector dominance contributions. They are illustrated by the following diagrams:

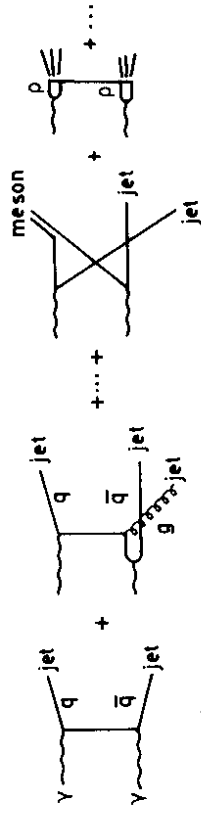


Diagram 6

For all but the first of these diagrams, part of the available energy is emitted along the initial photon directions close to the beam line. Only the 2-jet events may transfer all the energy to transversely produced jets and therefore can be expected to dominate at large transverse momenta with respect to the line of collision of the initial photons. As in e^+e^- annihilation, the cross section of this quark exchange scattering process may be normalized to μ -pair production:

$$R_{\gamma\gamma} = \frac{\sigma(\gamma\gamma \rightarrow q\bar{q})}{\sigma(\gamma\gamma \rightarrow \mu^+\mu^-)} = 3 \sum_{i=u,d,s,c} \frac{e_i^4}{27}$$

The question of interest is: does the experimental 2-jet cross section approach this number? and if so, can we learn something about the quark charges, the quark propagator, and the QCD behaviour?

The 2-jet cross section depends on the minimum transverse momentum required for jets. For the above value of $R_{\gamma\gamma}$ the inclusive jet cross section has been estimated³⁹⁾ to be:

$$\begin{aligned} \sigma(e^+e^- \rightarrow e^+e^- + \text{JET} + X) \\ \propto R_{\gamma\gamma} \frac{32\pi\alpha^2}{3(P_{T,\text{MIN}}^{\text{JET}})^2} \left(\frac{\alpha}{2\pi} \ln \frac{E_B}{m_e}\right)^2 \ln \frac{E_B}{P_{T,\text{MIN}}^{\text{JET}}} \\ \sim \frac{0.5\text{nb GeV}^2}{(P_{T,\text{MIN}}^{\text{JET}})^2} \sim 0.1 \text{ nb for } P_{T,\text{MIN}}^{\text{JET}} \gtrsim 2 \text{ GeV at } E_B = 15 \text{ GeV.} \end{aligned}$$

Typical 2-jet events are not back-to-back but kinked as shown in Fig. 14 for an event with a tagged electron in the JADE detector. Charged tracks (solid lines) are seen by the inner drift chambers and photons (dotted lines) - mostly from π^0 decays - are obtained from clusters in the lead glass shower counters.

For a proper analysis of hard scattering processes one has to employ jet search methods similar to those used in e^+e^- annihilation. The TASSO collaboration⁴⁰⁾ has analysed single tag events by applying the twoplicity method to the charged hadrons in the final state. The twoplicity method, which maximizes the momentum sums along two independent directions, forces all particles into two separate groups. If the transverse momenta of these groups exceed 2 GeV, they are used to experimentally define jets and these data are plotted in Fig. 15. As one can see, the vector dominance model calculation falls short of the data points, but the quark exchange contribution involving

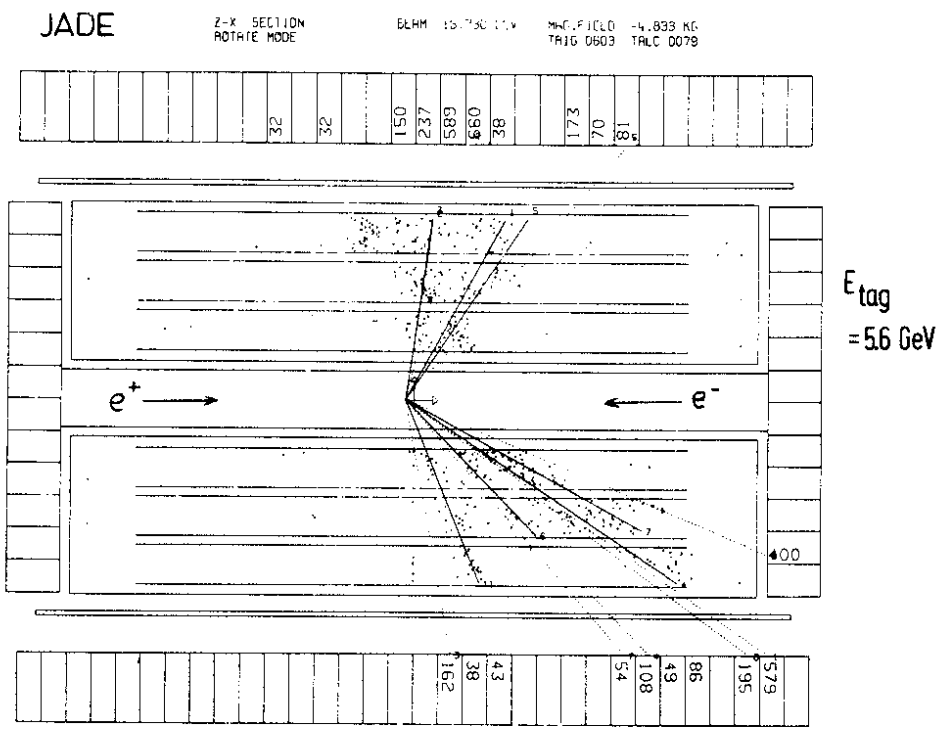
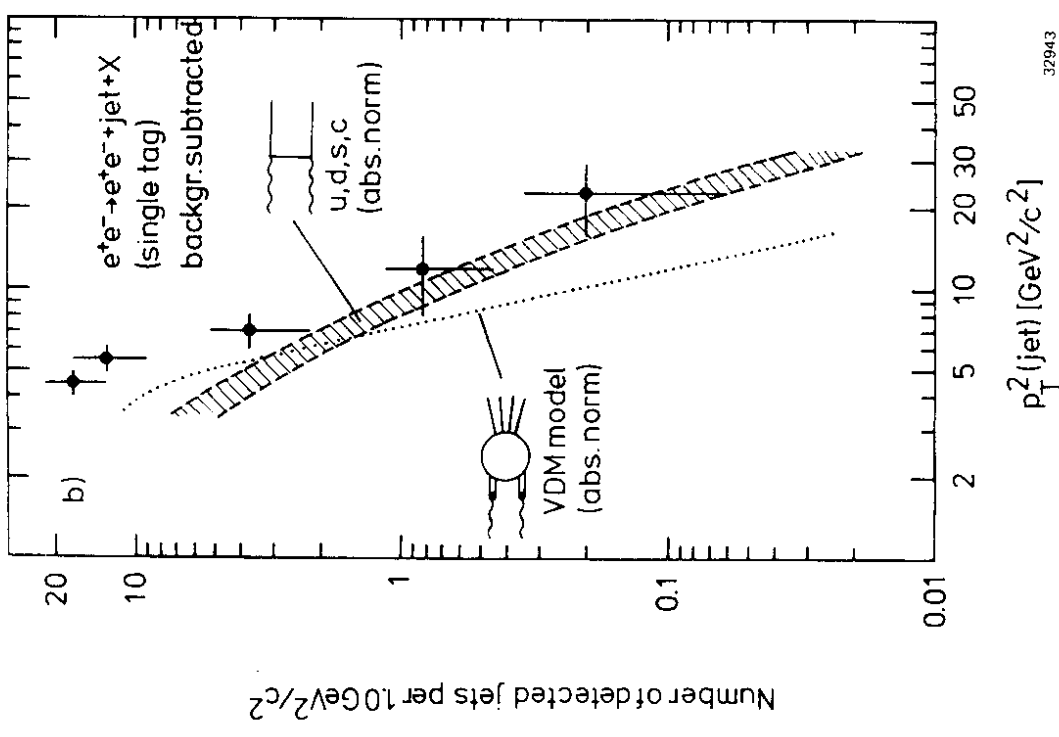


Fig. 14:
2-jet event with a tagged electron of 5.6 GeV seen in the JADE detector. Full lines are charged particles and dotted lines are photons.

32648



32943

Fig. 15: $p_T^2(\text{JET})$ distribution from TASSO for $e^+e^- \rightarrow e^+e^- + \text{jet} + X$ compared to a $e^+e^- \rightarrow e^+e^- + \bar{q}q$ model with four different types of normalization (shaded area) and to VDM (dotted line).

u, d, s, and c quarks is approached by the data for high transverse momenta.

For the JADE experiment⁴¹⁾ single tag events were analysed and the charged particles and photons in the final state were grouped according to a cluster search method⁴²⁾. The cluster search collects particles in well defined cones and has been extensively tested for e^+e^- annihilation events. This method allows for an arbitrary number of clusters and for single stray particles not assigned to any cluster. In order to qualify as jets the clusters have to have momenta of at least 2 GeV. For the 2-jet events obtained in this way, the jet transverse momenta exceeding 2 GeV are plotted in Fig. 16. The detector acceptance has been unfolded in order to obtain cross section values. The curve, representing the pointlike cross section normalized via the u, d, s, and c quark charges, displays the expected P_T^{-4} dependence and is approached by the data from above as the transverse momentum increases.

From the above discussion it is evident that the experimentally determined $R_{\gamma\gamma}$ is a function of the cut-off transverse momentum $P_{T,MIN}^{JET}$. Whereas JADE and TASSO tag electrons with Q^2 values of the order 0.3 GeV², the MAC experiment detects electrons over a wide angular range. Without requiring any cut-off in the jet momentum, the MAC group⁴³⁾ plots the ratio of observed hadronic to μ -pair events as function of Q^2 in Fig. 17 and obtains a surprisingly good agreement with the quark model prediction.

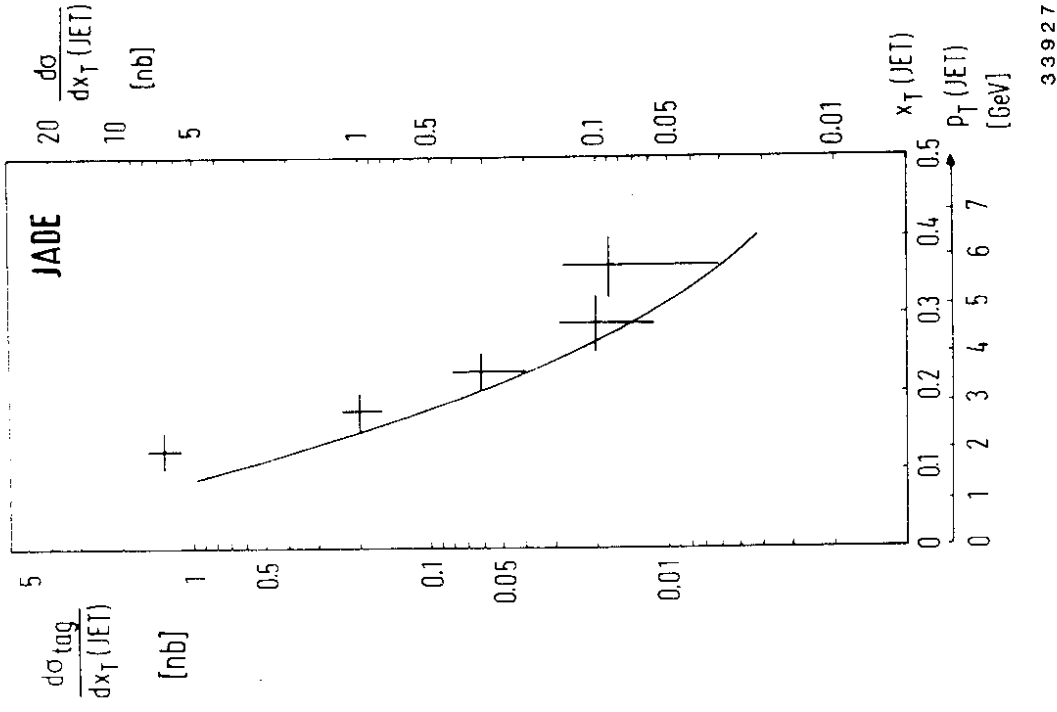


Fig. 16: Differential cross section for 2-jet events from JADE.
 $x_T(JET) = P_T(JET)/E_B$

**R' : TOTAL SINGLE TAG HADRONIC CROSS SECTION
TOTAL SINGLE TAG μ PAIR CROSS SECTION**

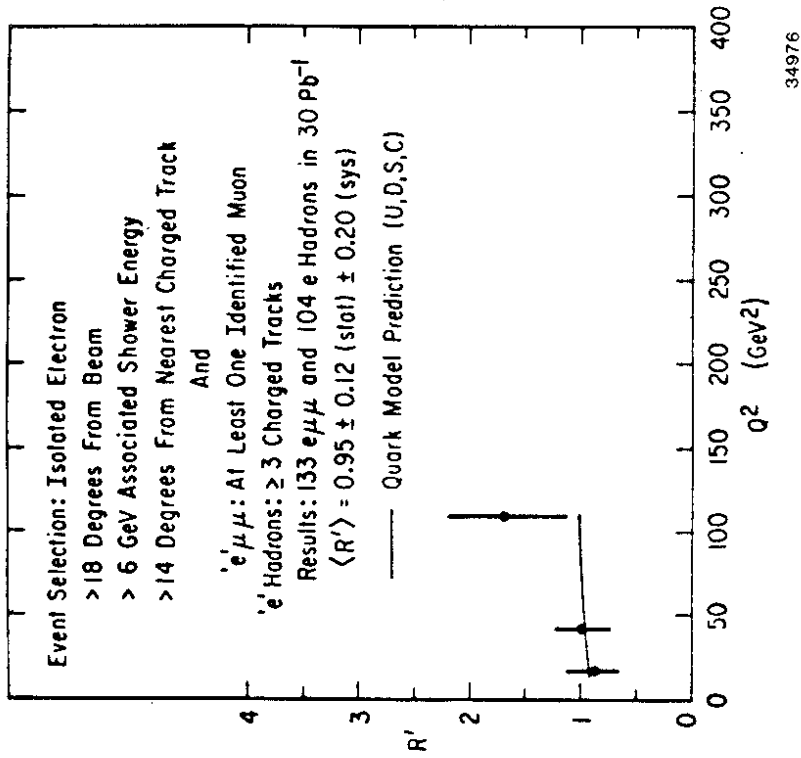


Fig. 17: Ratio of hadronic to μ -pair single tag events from MAC.

Early results on two-photon events of high invariant mass (W above 5 GeV) point at hard scattering processes. However, the data are too preliminary to allow any detailed comparison with QCD predictions or to test the quark propagator. It is an interesting feature that the $R_{\gamma\gamma}$ value of $\frac{34}{27}$ refers to fractional charged Gell-Mann-Zweig quarks⁴⁴⁾ and has to be changed to $\frac{10}{3}$ for integer charged Han-Nambu quarks⁴⁵⁾. Consequently, for integer charged quarks the curve of Fig. 16 has to be scaled up by a factor of 2.65, with the data points at high P_T starting to fall below this curve. This seems to rule out the scheme of Han-Nambu quarks, but it has been pointed out recently⁴⁶⁾ that for photons off mass-shell ($Q^2 \sim 0.3 \text{ GeV}^2$ for tagged electrons at JADE) the charges may be screened and the effect reduced.

Summary

The present situation in two-photon physics may be summarized

as follows:

- There are many new and nice results on resonances but no surprises.
- The glueballs, if they exist at all, seem to be below the level of detection efficiency of present experiments.
- The two-body final states $\pi^+\pi^-$, $\rho^+\rho^-$, $\bar{p}p$ show large cross sections near threshold.
- In deep inelastic ey scattering the photon structure function looks pointlike at modest Q^2 values.
- The observation of high P_T 2-jet events points at quark exchange scattering.

Acknowledgement

I have to thank my colleagues H. Kolanoski, T. Nozaki, J. Olsson, and T. Walsh for useful discussions.

References

- 1) H. Terazawa, Rev. Mod. Phys. 45 (1973) 615.
V.M. Budnev et al., Phys. Rep. 15C (1975) 182.
- 2) S.J. Brodsky et al., Phys. Rev. D4 (1971) 1532.
C. Carimalo et al., Phys. Rev. D20 (1979) 1057.
- 3) G. Barbiellini et al., PEP 1975 Summer Study (PEP 178) p. 159.
- 4) PLUTO Collaboration, Ch. Berger et al., Phys. Lett. 89B (1979) 120.
E. Hilger, DESY Report 80/75.
PLUTO Collaboration, Ch. Berger et al., Phys. Lett. 99B (1980) 287.
Ch. Berger, Proceed. 4th Intern. Coll. on $\gamma\gamma$ Interactions 1981, (Paris) p. 75.
- 5) C. Carimalo et al., Phys. Rev. D21 (1980) 669, and Proceed. Workshop on $\gamma\gamma$ Collisions (Amiens, 1980) p. 181.
- 6) G. Bonneau et al., Nucl. Phys. B54 (1973) 573.
J.H. Field, Nucl. Phys. B168 (1980) 477 and erratum B176 (1980) 545.
Ch. Berger and J.H. Field, Nucl. Phys. B187 (1981) 585.
- 7) D.J. Burke, Proceed. 4th Intern. Coll. on $\gamma\gamma$ Interactions 1981, (Paris) p. 123.
E. Hilger, Proceed. 4th Intern. Coll. on $\gamma\gamma$ Interactions 1981, (Paris) p. 149.
- 8) R.J. Medemeyer, Proceed. 1981 Intern. Symp. on Lepton and Photon Interactions at High Energies (Bonn) p. 410.
J. Olsson, Proceed. XVIIth Rencontre de Moriond 1982, (Les Arcs, Savoie) p. 13.
- 9) TASSO Collaboration, private communication
- 10) JADE Collaboration, Contribution to XXIst Intern. Conf. on High Energy Physics 1982 (Paris).
- 11) JADE Collaboration, private communication.
- 12) TASSO Collaboration, M. Althoff et al., DESY 82-071, to be published.
- 13) J.D. Bjorken, Proceed. Intern. Conf. on High Energy Physics 1979 (Geneva) p. 245.
S. Meshkov, Proceed. Orbis Scientiae 1980 (Coral Gables) p. 43.
S. Chanowitz, SLAC Summer Institute 1981 (SLAC-245) p. 41.
- 14) S. Okubo, Phys. Lett. 5 (1963) 105.
G. Zweig, CERN Report 8182/TH.401 (1964).
J. Iizuka et al., Progr. Theor. Phys. 35 (1966) 1061.
- 15) Crystal Ball Collaboration, C. Edwards et al., Phys. Rev. Lett. 48 (1982) 458.
MARK II Collaboration, D.L. Burke et al., Phys. Rev. Lett. 49 (1982) 632.
- 16) Mark II Collaboration, Contribution to XXIst Intern. Conf. on High Energy Physics 1982 (Paris).

- 17) K. Koller and T.F. Walsh, Nucl. Phys. B140 (1978) 449.
T. Walsh, Proceed. Intern. Symp. on High Energy e^+e^- Interactions, Vanderbilt 1980 (Nashville, AIP No. 62) p. 14.
- 18) H.J. Schnitzer, Nucl. Phys. B207 (1982) 131.
- 19) J.L. Rosner, Phys. Rev. D24 (1981) 1347, and "Quark content of neutral mesons" (preprint, 1982).
- 20) TASSO Collaboration, Contribution to XXIst Intern. Conf. on High Energy Physics 1982 (Paris), and DESY 82-073.
- 21) ACCMOR Collaboration, C. Daum et al., Phys. Lett. 104B (1981) 246.
- 22) A. Etkin et al., Contribution to XXIst Intern. Conf. on High Energy Physics 1982 (Paris), and Phys. Rev. Lett. 49 (1982) 1620.
- 23) D.L. Scharre, Proceed. Orbis Scientiae 1982 (Coral Gables), and SLAC-PUB-2880.
- 24) TASSO Collaboration, M. Althoff et al., DESY 82-062, to be published.
- 25) TASSO Collaboration, R. Brandelik et al., Phys. Lett. 108B (1982) 67.
- 26) P.H. Dangaard, preprint CLNS-81/519 (Cornell Univ., 1981).
- 27) I.F. Walsh, Phys. Lett. 36B (1971) 121.
- 28) C. Peterson et al., Nucl. Phys. B174 (1980) 424.
- 29) T.F. Walsh and P. Zerwas, Phys. Lett. 44B (1973) 195.
- 30) E. Witten, Nucl. Phys. B120 (1977) 189.
C.H. Llewellyn Smith, Phys. Lett. 79B (1978) 83.
C.T. Hill et al., Nucl. Phys. B148 (1979) 373.
R.J. Dewitt et al., Phys. Rev. D19 (1979) 2046.
W.R. Frazer and J.F. Gunion, Phys. Rev. D20 (1979) 147.
- 31) W.A. Bardeen and A.J. Buras, Phys. Rev. D20 (1979) 166.
D.W. Duke and J.F. Owens, Phys. Rev. D22 (1981) 2280.
T. Uematsu and I.F. Walsh, Phys. Lett. 101B (1981) 263.
- 32) T. Uematsu and I.F. Walsh, Nucl. Phys. B199 (1982) 93.
- 33) E. 8loom et al., Phys. Rev. D5 (1972) 528.
M. Breidenbach and J. Kuti, Phys. Lett. 41B (1972) 234.
W.A. Atwood et al., Phys. Lett. 64B (1976) 479.
A. Bodek et al., Phys. Rev. D20 (1979) 1471.
- 34) CELLO Collaboration, Contribution to XXIst Intern. Conf. on High Energy Physics 1982 (Paris).
- 35) PLUTO Collaboration, Ch. Berger et al., Phys. Lett. 107B (1981) 168.
- 36) JADE Collaboration, W. Bartel et al., DESY 82-064, to be published.
- 37) W.A. Bardeen et al., Phys. Rev. D18 (1978) 3998.
- 38) W.R. Frazer, Proceed. 4th Intern. Coll. on $\gamma\gamma$ Interactions 1981 (Paris) p. 101.
W.A. Bardeen, Proceed. 1981 Intern. Symp. on Lepton and Photon Interactions at High Energies (Bonn) p. 432.
- 39) S. Brodsky et al., Phys. Lett. 41 (1978) 672, and Phys. Rev. D19 (1979) 1418.
K. Kajantie, Phys. Scr. 29 (1979) 230, and Acta Phys. Austriaca, Suppl. XXI (1979) 663.
K. Kajantie and R. Raitio, Nucl. Phys. B159 (1979) 528.
- 40) TASSO Collaboration, R. Brandelik et al., Phys. Lett. 107B (1981) 290.
- 41) JADE Collaboration, W. Bartel et al., Phys. Lett. 107B (1981) 163.
- 42) H.J. Daum et al., Zeitschr. Phys. C8 (1981) 167.
- 43) MAC Collaboration, private communication.
- 44) M. Gell-Mann, Phys. Lett. 8 (1964) 214.
G. Zweig, CERN Report 84197TH. 412 (1964).
- 45) M.Y. Han and Y. Nambu, Phys. Rev. 139B (1965) 1006.
Y. Nambu and M.Y. Han, Phys. Rev. D10 (1974) 674.
J.C. Pati, Proceed. Intern. Summer Institute on Theor. Particle Physics (Hamburg, 1975) p. 384.
H.K. Lee, preprint IC/78/95 (Trieste, 1978).
- 46) T. Jayaraman et al., preprint MUTP-82/3 (Madras, 1982), and Phys. Lett. 119B (1982) 215.